

# RSC Advances

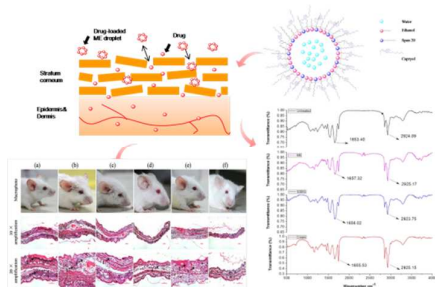


This is an *Accepted Manuscript*, which has been through the Royal Society of Chemistry peer review process and has been accepted for publication.

*Accepted Manuscripts* are published online shortly after acceptance, before technical editing, formatting and proof reading. Using this free service, authors can make their results available to the community, in citable form, before we publish the edited article. This *Accepted Manuscript* will be replaced by the edited, formatted and paginated article as soon as this is available.

You can find more information about *Accepted Manuscripts* in the [Information for Authors](#).

Please note that technical editing may introduce minor changes to the text and/or graphics, which may alter content. The journal's standard [Terms & Conditions](#) and the [Ethical guidelines](#) still apply. In no event shall the Royal Society of Chemistry be held responsible for any errors or omissions in this *Accepted Manuscript* or any consequences arising from the use of any information it contains.



Topical administration of the optimal microemulsion could effectively enhance skin location amount of azelaic acid without causing skin irritation.

1 **Improved percutaneous delivery of azelaic acid employing microemulsion as**  
2 **nanocarrier: Formulation optimization, *in vitro* and *in vivo* evaluation**

3 Huixian Ma<sup>a</sup>, Meng Yu<sup>a</sup>, Fengping Tan<sup>a\*\*</sup>, Nan Li<sup>a\*</sup>

4  
5  
6  
7  
8  
9 <sup>a</sup>Tianjin Key Laboratory of Drug Delivery and High-Efficiency, School of  
10 Pharmaceutical Science and Technology, Tianjin University, 300072 Tianjin, PR  
11 China

12  
13  
14  
15 \*Corresponding author at: School of Pharmaceutical Science and Technology, Tianjin  
16 University, 300072, Tianjin, PR China.

17 E-mail address: [linan19850115@163.com](mailto:linan19850115@163.com)

18 Tel.: +86-022-27404986

19 \*\* Co-corresponding author at: School of Pharmaceutical Science and Technology,  
20 Tianjin University, 300072, Tianjin, PR China.

21 E-mail address: [tanfengping@163.com](mailto:tanfengping@163.com)

22 Tel.: +86-022-27405160

23

24

25

26 **Abstract:** The present study aimed to develop and optimize a microemulsion (ME)  
27 nanocarrier system as topical vehicle of azelaic acid (AZA) to improve its skin  
28 location and therapeutic efficacy. D-optimal mixture experimental design was utilized  
29 to optimize ME for realizing maximum skin retention and appropriate droplet size.  
30 Three formulation variables: Smix X1 (a mixture of Span 20/Ethanol, 1:9, w/w),  
31 water X2 and Oil X3 (Capryol 90) were included in the design; while the three  
32 responses contained skin retention (Y1), AZA amount in collection medium after 24 h  
33 (Y2) and mean particle size (Y3). The values of formulation components (X1, X2 and  
34 X3) were 50.3%, 13.5% and 36.2%, respectively. *In vitro* studies, the optimal  
35 ME revealed much higher release rate, enhanced skin targeting and  
36 penetration effect of AZA relatively to control formulations (ethanol  
37 solution based gel and commercial cream). Attenuated total reflectance  
38 fourier-transform infrared spectroscopy study further confirmed us that  
39 vehicles could transport the active agents across stratum corneum (SC)  
40 layer by changing the amount and arrangement of lipid within SC. In addition,  
41 skin irritation test and pharmacodynamics studies were conducted, and the results  
42 suggested that the optimal ME exhibited prominent therapeutic effect over control  
43 formulations without any irritant response.

44 **Keywords:**

45 Azelaic acid; microemulsion; formulation optimization; skin targeting effect;  
46 therapeutic efficacy.

47

## 48 1. Introduction

49 Rosacea is a common chronic inflammatory dermatosis characterized by  
50 transient or persistent central facial erythema, visible blood vessels, and often papules  
51 and pustules.<sup>1</sup> The cause of rosacea is still unknown, however, available evidence  
52 supports that genetic and environmental factors (such as sun exposure, drinking  
53 alcohol, and cosmetics) should be responsible for the etiology of this skin disorder.<sup>2</sup>  
54 Rosacea affects mostly facial skin which leads to the much trouble on the social  
55 contact of suffers in a prominent manner.<sup>3</sup> Moreover, the current treatment of rosacea  
56 has been claimed to be empiric and imperfect.

57 Azelaic acid (1,7-heptanedicarboxylic acid, AZA) is a saturated, straight-chained  
58 C9-dicarboxylic acid that has been reported to be the active pharmaceutical ingredient  
59 in a number of prescription drugs for the treatment of rosacea.<sup>4</sup> AZA, however, with  
60 its commercial formulations of 15% gel (FINACEA<sup>®</sup>) and 20% cream (Skinoren<sup>®</sup>),  
61 restrains its penetration across the stratum corneum (SC) due to poor bioavailability  
62 mainly caused by low drug dissolved fraction and poor skin permeability.<sup>2,5</sup>  
63 Theoretically, suitable percutaneous permeation is an essential factor for  
64 pharmaceutical agents to achieve satisfactory therapeutic effect. Topical delivery  
65 systems aiming to promote AZA cutaneous penetration are necessary to maximize its  
66 biological efficacy. Meanwhile, considering the local nature of skin disorders, it is  
67 advisable to reside drug at the site of application for localized delivery.

68 Effective penetration of the active agents through the SC is a major challenge in  
69 topical drug delivery.<sup>6</sup> On the matter a number of research works have been done to

70 increase skin penetration through the SC, such as chemical modification,<sup>7</sup> penetration  
71 enhancer or retardant,<sup>8</sup> micro-needles,<sup>9</sup> and microwaves.<sup>10</sup> Recently, nanoscale  
72 vehicles have attracted significant attention as delivery strategies for active molecules,  
73 e.g. liposomes,<sup>11</sup> solid lipid nanoparticles,<sup>12</sup> and microemulsion.<sup>13,14,15,16</sup>

74 Microemulsion (ME) has been proved to have a significant potential to increase  
75 the penetration of lipophilic, hydrophilic, and amphiphilic substances into and  
76 through the skin compared to conventional vehicles.<sup>17,18</sup> MEs are optically isotropic  
77 and thermodynamically stable nanosized structure mixtures of aqueous phase, oil  
78 phase and amphiphile(s).<sup>19,20</sup> Several mechanisms have been proposed to explain the  
79 advantages of ME superior to conventional vehicles. First, the ingredients of ME  
80 could interfere the diffusional barrier of the SC and improve cutaneous permeation of  
81 drug by acting as permeation enhancers.<sup>13</sup> Second, the increased thermodynamic  
82 activity of drugs incorporated in ME formulations is a significant driving force for  
83 drug release and skin penetration.<sup>21</sup> Third, small droplet size could settle down to  
84 close contact with the skin which leads to a considerable increase of surface area and  
85 hence improves absorption.<sup>22</sup> Also, continuously and spontaneously fluctuating  
86 interface of ME enables high drug mobility and subsequently enhances drug diffusion  
87 process.<sup>23</sup>

88 The aim of this work was to optimize a ME nanocarrier system for AZA, which  
89 provided skin targeting effect and maximum dermal therapeutic effect. ME  
90 formulations were developed by constructing pseudo-ternary phase diagrams and  
91 optimized by D-optimal design based on maximum drug amount in skin layers,

92 appropriate skin penetration and small particle size. The optimized formulation was  
93 characterized by droplet size, size distribution and pH value. Attenuated total  
94 reflectance fourier transform infrared spectroscopy (ATR-FTIR) study was carried out  
95 to elucidate the interaction mechanism between ME and skin. Besides, the optimized  
96 ME formulations, ethanolic solution based gel and commercial cream were evaluated  
97 for *in vitro* skin permeation studies, skin sensitivity test, and pharmacodynamics study  
98 for comparison purpose.

## 99 **2. Materials and Methods**

### 100 **2.1. Materials**

101 Azelaic acid (MW 188, 99% purity) was purchased from Huabei reagent Co., Ltd  
102 (Tianjin, China). Capryol<sup>®</sup> 90 with a purity of 98% was a kind gift from Gattefossé  
103 (Saint-Priest, France). Ethanol (99% purity) and Span 20 (with a purity of 98%) were  
104 obtained from Jiangtian pharmaceutical reagent Co., Ltd (Tianjin, China). Klucel<sup>®</sup>  
105 MF was purchased from Hercules, Inc. (Wilmington, DE, USA). 20% AZA  
106 commercial cream (Skinoren<sup>®</sup>) was obtained from Bayer Co., Ltd (Taiwan). All  
107 other reagents were of analytical grade.

### 108 **2.2. Skin membranes and animals**

109 The abdominal porcine skin was obtained from pig less than one month old.  
110 After removing the hair and the subcutaneous tissue, the skin was washed with normal  
111 saline, divided into small pieces and stored at - 20 °C until use. Wistar rats (about  
112 200 ± 20 g) and Male Kun-Ming mice (weighing 20 ± 2 g) were purchased from  
113 Chinese Academy of Medical Sciences (Tianjin, China) and used for skin irritation

114 test and *in vivo* therapeutic effects of anti-rosacea, respectively. All work performed  
115 with animals was in accordance with and approved by the Institutional Animal Care  
116 and Use of Tianjin University.

### 117 **2.3. Construction of pseudo-ternary phase diagram and preparation of** 118 **formulations**

119 The pseudo-ternary phase diagram was constructed based on the oil phase  
120 (Capryol 90), surfactant (Span 20), cosurfactant (ethanol) and water. The mass ratio of  
121 surfactant to cosurfactant (Smix) was fixed at 1:9. Then, the oil phase was mixed with  
122 Smix at w/w ratios ranging from 1:9 to 9:1. Finally, 1 g of oil/Smix mixture in  
123 appropriate ratio was titrated with water drop by drop under magnetic stirring at  
124 ambient temperature. The resultant mixtures were examined according to their visual  
125 appearance. Usually, the system which was a transparent and low viscous solution  
126 was defined as ME region. In contrast, the turbid sample was identified as  
127 conventional emulsion. The boundary point between ME region and emulsion region  
128 was determined and corresponding component ratio was recorded to plot the  
129 pseudo-ternary phase diagram.

130 When preparing drug-loaded ME formulations, 10% (w/w) AZA was dissolved  
131 in the oil/Smix mixture. Then, appropriate amount of water was added to prepare ME  
132 formulations under magnetic stirring.

133 An ethanolic solution based gel (ESBG) containing the same AZA concentration  
134 (10%, w/w) was prepared and utilized as control formulation. Klucel<sup>®</sup> MF was added  
135 to bidistilled water under stirring until complete incubation. The obtained gel was



136 diluted with equal amount of ethanol solution followed by the addition of AZA,  
137 resulting in a final AZA concentration of 10% (w/w).

#### 138 **2.4. Formulation optimization of AZA-loaded MEs**

139 D-optimal mixture experimental study was designed based on a three component  
140 system: Smix X1 (a mixture of Span 20/ethanol, 1:9, w/w), aqueous phase X2 (water)  
141 and the oil phase X3 (Capryol 90). The total concentration of the three components  
142 summed to 100%. Based on the obtained ME region in the phase diagram, the range  
143 of each component was selected as follows: X1 (40-80%), X2 (0-30%), and X3  
144 (20-60%) (This district was shown in Fig. 1). The skin retention amount of AZA at 24  
145 h (Y1), AZA amount in collection medium after 24 h (Y2) and mean particle size (Y3)  
146 were used as the responses (dependent variables). The responses of all model  
147 formulations were treated with Design-Expert software (version 7; Stat-Ease, Inc,  
148 Minneapolis, MN). Suitable models for D-optimal design containing linear, quadratic,  
149 special cubic and cubic models. The best fitting mathematical model was selected by  
150 comparing statistical parameters including the standard deviation (SD), the multiple  
151 correlation coefficient ( $R^2$ ), adjusted multiple correlation coefficient (adjusted  $R^2$ ) and  
152 the predicated residual sum of square (PRESS), proved by Design-Expert software.  
153 Since the PRESS value indicated how well the model fits the data, the value  
154 of the selected model should be smallest among these models.<sup>24</sup> The base  
155 design consisted of 16 runs (Table 1).

#### 156 **2.5. Evaluation of prepared formulations**

157 Malvern Mastersizer (Nano ZS90, Malvern Instruments, Malvern, UK) was

158 used for determining of droplet size for D-optimal design. The optimized ME  
159 formulation was characterized for droplet size, size distribution profile and zeta  
160 potential. The pH values of the optimized ME formulation, ESG and marketed  
161 cream were detected using a digital pH-meter (PHS-3C, Shenbang Instrument  
162 Corporation, Shanghai, China) at  $25 \pm 2$  °C.

### 163 **2.6. Stability assay**

164 The optimal AZA loaded ME was preserved in glass vial with a sealing  
165 cap and was kept under long-term condition at  $25 \pm 2$  °C/ $60 \pm 5\%$  RH. The  
166 physical stability of the ME formulation was assessed for appearance,  
167 droplet size and polydispersity index (PDI) at predetermined time  
168 interval of 0, 1, 2, and 3 months. For chemical stability, concentration  
169 of AZA in the ME was determined by HPLC analysis at each predetermined  
170 time interval.

### 171 **2.7. *In vitro* skin permeation studies**

172 Porcine skin samples were mounted on Franz Diffusion Cells with the SC side  
173 facing the donor chamber (diffusion area =  $1.77$  cm<sup>2</sup>). The receptor medium was  $17.6$   
174 mL of normal saline under constant magnetic stirring at  $500$  rpm. After equilibration  
175 of skin samples with normal saline for  $1$  h at  $37 \pm 0.5$  °C, finite doses ( $25$  mg cream  
176 and  $50$  mg of the optimal ME formulation and ESG, which correspond to  $5$  mg AZA,  
177 respectively) were applied to skin surface ( $n = 6$ ). At predetermined time intervals ( $4$ ,  
178  $6$ ,  $8$ ,  $10$ ,  $12$  and  $24$  h), approximately  $0.5$  mL of the receptor medium was withdrawn  
179 for HPLC analysis and equal volume of fresh normal saline was compensated. The

180 remaining formulation on the skin surface was wiped with cotton ball soaked with  
181 methanol/water (40/60, v/v) after incubation for 24 h. The tape-stripping method was  
182 employed to remove SC layer.<sup>22</sup> The skin was stripped with 15 pieces of adhesive tape  
183 and all the tapes except for the first one were digested with methanol/water (40/60,  
184 v/v), then filtered for analysis. After removal of SC, the remaining skin samples were  
185 minced, vortexed with 5 mL of methanol and centrifuged to extract residual AZA in  
186 the epidermis and dermis. The supernatants were collected and filtered for analysis.  
187 The permeation rate of AZA (flux,  $\mu\text{g}/\text{cm}^2 \text{ h}$ ) through porcine skin was calculated  
188 from the slope of linear portion of the cumulative amount permeated through the skins  
189 per unit area versus time plot.

## 190 **2.8. HPLC method**

191 A Water e2695 series HPLC with UV 2489 detector (Waters, USA) was used for  
192 AZA method validation. The optimized chromatographic conditions were present as  
193 follows: 250 mm  $\times$  4.6 mm stainless steel C18 column (I.D., 5  $\mu\text{m}$ , Thermo, USA);  
194 column temperature at 35  $^{\circ}\text{C}$ ; 20  $\mu\text{l}$  injection volume; detection wavelength set at 215  
195 nm; mobile phase consisted of acetonitrile and phosphate buffer (pH 3.0, 50 mM) at  
196 25:75 (v/v); flow rate of 1.0 ml/min.

197 For in vitro studies, the peak area (y) correlated linearly with AZA  
198 concentration (x,  $\mu\text{g}/\text{ml}$ ) in the range of 5.0 - 100.0  $\mu\text{g}/\text{ml}$  with a mean  
199 correlation coefficient of 0.9999. The regression equation of the  
200 calibration curve was  $y = 586.54x - 317.69$  with recovery of 99.36%.

## 201 **2.9. Attenuated total reflectance fourier transform infrared**

**202 spectroscopy (ATR-FTIR) study**

203 To prepare SC sample for ATR-FTIR study, the SC was firstly separated by  
204 placing the skin sample in 0.5% trypsin (type I, Sigma Aldrich) in phosphate-buffered  
205 saline pH 7.4 for 4 h.<sup>25</sup> The obtained SC sheet was cleaned with deionized water and  
206 dried in desiccator for 12 h. Then, the SC samples were incubated with different  
207 formulations by means of diffusion cells for 24 h as section 2.6 described. All  
208 experiments were performed in triplicate. The samples were mixed with KBr to make  
209 pellets and were measured on an FTIR spectrometer (Bruker EQUINOX, Germany)  
210 with a spectral resolution of 4 cm<sup>-1</sup>. The absorbance was measured in the region from  
211 400 cm<sup>-1</sup> to 4000 cm<sup>-1</sup> at 37 °C.

**212 2.10. Skin irritation test**

213 To determine the skin compliance of the developed formulations, skin  
214 irritation test was carried out based on histopathological examination.  
215 The hair on the dorsal side (2 cm × 3 cm) of Wistar rats was carefully  
216 removed without damaging the skin.<sup>26</sup> The control group was treated with  
217 normal saline while other groups were treated with the optimized ME  
218 formulation, ESGG and commercial cream (containing 5 mg of AZA),  
219 respectively, three times a day for three days consecutively (n = 3). These  
220 formulations were uniformly spread within the area of 1.77 cm<sup>2</sup>. After 3  
221 days, the animals were observed for any signs of itching or change in skin  
222 such as erythema, papule, and dryness. Then, the rats were sacrificed using  
223 carbon dioxide gas. The test skin was removed, fixed and stored in

224 formaldehyde (10%, v/v). Tissue specimens were processed routinely and  
225 embedded in paraffin wax. Paraffin blocks were cut serially at 10  $\mu\text{m}$ .  
226 Sections were stained with hematoxylin and eosin (H&E) and examined by  
227 light microscope (Olympus BX-51, Japan).

## 228 **2.11. Pharmacodynamics studies**

229 Croton oil inflammation model was performed to induce rosacea model.<sup>27,28</sup>  
230 Briefly, 10  $\mu\text{L}$  of croton oil in acetone (5% v/v) was painted on the inner surface of  
231 the right ears in group a-e, while the left ears were used as control. Fifteen minutes  
232 later, 60  $\mu\text{L}$  of blank ME, AZA-loaded ESBG (10%, w/w) and AZA-loaded ME (10%,  
233 w/w) were topically applied to group b, c, d, respectively. Commercial cream (20%,  
234 25 mg) was administrated to group e. At 4, 8 and 24 h, ear thickness was measured  
235 near the top of the ear distal to the cartilaginous ridges. Change in ear thickness from  
236 control was taken as an edema index. The ear tissue samples were collected after 24 h  
237 and submitted to histopathological analysis.

## 238 **2.12. Data analysis**

239 At least three to six replicates of each experiment were used. All results were  
240 reported as mean  $\pm$  SD. Paired two-tailed Student's t-test was employed to calculate  
241 the statistical significance. The level of significance was set as  $p < 0.05$ .

## 242 **3. Results and discussion**

### 243 **3.1. Construction of pseudo-ternary phase diagram**

244 Pseudo-ternary phase diagrams were constructed to determine the components  
245 and concentration range for ME. Based on the optimization study of pseudo-ternary

246 phase diagrams in our lab (unpublished data), the optimized pseudo-ternary phase  
247 diagram is shown in Fig. 1. The ME region was observed near the surfactant vertex  
248 characterized by high surfactant content and low water content. In other words,  
249 water-in-oil (W/O) MEs were easily formed at high Smix content. The maximal  
250 water solubilization capacity of this W/O system was nearly 40%, which  
251 might be ascribed to the excellent intersolubility of water and ethanol.  
252 Different ME formulations in the area surrounded by blue lines were prepared and  
253 optimized based on D-optimal design.

### 254 **3.2. Formulation optimization of MEs using D-optimal design**

255 D-optimal design is an efficient method for the optimization of pharmaceutical  
256 formulations, which could clarify the relationship between independent variables and  
257 dependent variables in a formulation. In our study, D-optimal mixture experimental  
258 design was conducted to rapidly obtain the optimal ME formulation. Smix (a mixture  
259 of Span 20/ethanol, 1:9, w/w) (X1), water (X2) and Capryol 90 (X3) were chosen as  
260 formulation variables, at the mean time the skin retention (Y1), AZA amount in  
261 collection medium after 24 h (Y2) and mean particle size (Y3) were selected as  
262 responses (dependent variables). The responses of these formulations were  
263 summarized in Table 1.

264 The independent and response variables were related using polynomial  
265 equation with statistical analysis through Design-Expert software  
266 (version 7; Stat-Ease, Inc, Minneapolis, MN). The equation that fitted  
267 to the data was as follows:

$$\begin{aligned} 268 \quad Y &= b_1X_1 + b_2X_2 + b_3X_3 + b_4X_1X_2 + b_5X_1X_3 + b_6X_2X_3 + b_7X_1X_2X_3 + b_8X_1X_2(X_1-X_2) \\ 269 \quad &+ b_9X_1X_3(X_1-X_3) + b_{10}X_2X_3(X_2-X_3) \end{aligned} \quad (1)$$

270 where  $b_1$  to  $b_{10}$  are the coefficients computed from the observed experimental  
271 values of  $Y$ . Coefficients with one factor represents the effect of that  
272 particular factor while the coefficients with more than one factor  
273 represents the interaction between those factors. Positive sign in front  
274 of the factors indicates synergistic effects while negative sign  
275 indicates antagonistic effect of the factors.<sup>29</sup>

276 In our study, drug accumulation in skin layers was considered to be the most  
277 significant factor to evaluate the efficiency of formulations. As shown in Table 1, skin  
278 retention amount of AZA released from ME formulations varied from 111.49 to  
279 593.26  $\mu\text{g}$ , inferring that the three independent factors possessed a profound effect on  
280 AZA skin retention amount. The approximation of response values of  $Y_1$  based on Sp.  
281 cubic model was the most suitable due to its smallest PRESS value (Table 2). The  
282 related regression equation was:

$$\begin{aligned} 283 \quad Y_1 &= 204.20X_1 + 546.05X_2 + 111.33X_3 + 510.31X_1X_2 + 170.11X_1X_3 + \\ 284 \quad &314.46X_2X_3 + 5007.79X_1X_2X_3 \end{aligned} \quad (2)$$

285 The positive values of all coefficients confirmed the synergistic effect of the three  
286 independent variables on  $Y_1$ . Besides, it was obvious that the term  $X_1X_2X_3$  had the  
287 highest effect on this response with the largest coefficient of 5007.79, which could be  
288 confirmed by the 2D contour diagram that illustrated the effect of varying ratios of  $X_1$ ,  
289  $X_2$ , and  $X_3$  on the skin retention of MEs (Fig. 2a). As was indicated by the central

290 solid portion of the plot, ME formulations at moderate level of oil, Smix and water  
 291 could perform higher skin retention, which represented higher therapeutic efficacy.

292 The AZA amount in collection medium after 24 h (Y2) of the different ME  
 293 formulations ranged from 161.67 to 792.74  $\mu\text{g}$  (Table 1). As presented in Table 2,  
 294 quadratic model was the most appropriate mathematical model for Y2 with  
 295 obtained regression equation:

$$296 \quad Y = 217.90X_1 + 736.56X_2 + 230.15X_3 + 1048.47X_1X_2 + 290.91X_1X_3 +$$

$$297 \quad 337.94X_2X_3 \quad (3)$$

298 The coefficient of  $X_1X_2$  for this response was the largest one, indicating the positive  
 299 effect of combination of Smix and water content on the drug penetrated into the  
 300 receptor medium. From the 2D contour plots (Fig. 2b), we could observe that  
 301 moderate levels of three factors indicated relatively lower cumulative AZA amount in  
 302 receptor medium, which represented less systemic side effects. For mean particle size,  
 303 cubic model was the most suitable model based on the largest  $R^2$  value ( $R^2 = 0.9980$ ,  
 304 Table 2). The regression equation was presented as follows:

$$305 \quad Y = -0.034X_1 + 6.26X_2 + 0.020X_3 + 31.91X_1X_2 - 0.69X_1X_3 + 18.79X_2X_3 -$$

$$306 \quad 97.55X_1X_2X_3 - 15.26X_1X_2(X_1-X_2) - 5.20X_1X_3(X_1-X_3) + 38.89X_2X_3(X_2-X_3)$$

$$307 \quad (4)$$

308 According to 2D contour plots (Fig. 2c), the water content provided the largest  
 309 contribution to the mean droplet size. In other words, increasing amount of water  
 310 resulted in nonlinear escalations in particle size. In fact, mean droplet size of  
 311 formulations containing less than 4% water content as well as water-free systems



312 (mixtures of the surfactant, cosurfactant and oil, S/COS/O-mix) was not measurable.  
313 As water content increased, the droplet size of ME formulations also increased,  
314 indicating a swelling process taken place within the droplets at high aqueous  
315 contents.<sup>30</sup>

316 In order to obtain optimal ME formulations with maximum skin targeting effect  
317 and minimum skin permeation, the response Y1 should be maximized ( $> 600 \mu\text{g}$ )  
318 while Y2 should be minimized ( $< 600 \mu\text{g}$ ). The S/COS/O-mixtures resulted in  
319 significantly lower AZA permeation relative to ME droplets (Fig. 2a b), which  
320 demonstrated that the presence of droplets in nanosize had a prominent contribution to  
321 the percutaneous penetration of drugs.<sup>31</sup> Thus, the response Y3 should have optimal  
322 intermediate range (5-10 nm) to ensure the formation of ME droplets, resulting in  
323 maximum skin retention with less systemic side effects. Based on these conditions,  
324 the three responses were then combined to determine an all over optimum region (Fig.  
325 3). According to the selection criteria, an ME which satisfied with optimal drug skin  
326 retention, appropriate permeated amount of drug and droplet size was considered to be  
327 the optimal formulation. An optimal response was found with Y1, Y2 and Y3 of  
328 571.64  $\mu\text{g}$ , 573.97  $\mu\text{g}$  and 3.78 nm at X1, X2 and X3 value of 50.3%, 13.5% and  
329 36.2%, respectively (Table 3). In order to assess the reliability of the  
330 developed mathematical model, microemulsion formulation was formed  
331 corresponding to above mentioned factor levels. Experimental values of  
332 Y1, Y2 and Y3 were 593.57  $\mu\text{g}$ , 584.69  $\mu\text{g}$ , and 3.83 nm, respectively. The  
333 predicted and experimental values demonstrated small percentage error of 3.69%,

334 1.83% and 1.32%, respectively. In addition, a good agreement was obtained between  
335 the model prediction and experimental observation. The optimal ME formulation was  
336 used for next steps, while ethanolic solution based gel (ESBG) and 20% AZA  
337 commercial cream (Skinoren<sup>®</sup>, Bayer Co., Ltd, Taiwan) were used as control  
338 formulations.

### 339 **3.3. Evaluation of prepared formulations**

340 The appearance of the optimal ME was clear and transparent by visual  
341 observation (Fig. 4). The particle size, PDI value and zeta potential of the optimal ME  
342 were 3.83 nm, 0.216 and -4.99, respectively, ratifying its excellent homogeneity and  
343 stability. The pH values were determined as 3.44, 3.13 and 4.15 for cream, ESBG and  
344 ME, respectively (Table 4). Among the three formulations, the pH value of ME was  
345 consistent with that of human skin surface (typically slightly above pH = 5), resulting  
346 in less skin irritant potential to a certain degree.<sup>9</sup>

### 347 **3.4. Stability assay**

348 The optimized ME formulation was stable when stored at  $25 \pm 2$  °C/60  
349  $\pm$  5% RH for three months where there was no obvious change in visual  
350 appearance (Table 5). Besides, the main changes of droplet size and PDI  
351 were also not observed during 3 months. The concentration of AZA in the  
352 optimal ME was above  $98.69\% \pm 3.96$  during 3 months, which demonstrated  
353 that there was no degradation.

### 354 **3.5. *In vitro* skin permeation studies**

355 The penetration behaviors of AZA from the optimized ME, ESBG and

356 commercial cream were evaluated for comparison purpose. The cumulative permeated  
357 amount of AZA through porcine skin after 24 h was calculated and plotted against  
358 time. As shown in Fig. 5, the cumulative amount of AZA in the receptor chambers  
359 was steadily increased over time. The optimal ME and ESBG presented a comparable  
360 penetration behavior through the skin, which was significantly higher than that of  
361 AZA marketed cream ( $P < 0.05$  for ESBG;  $P < 0.01$  for ME). Moreover, the ME  
362 formulation and ESBG provided higher permeation rate than cream, which  
363 represented a possible rapid therapeutic effect. The results demonstrated that the  
364 tested ME formulation and ESBG had potent enhancement effect for the topical  
365 administration of AZA.

366 Drug accumulation in different skin layers (SC and viable skin layers) after 24 h  
367 application of the three formulations was determined (Fig. 6). The total skin retention  
368 was defined as the sum of the amounts in the SC and viable skin layers (epidermis and  
369 dermis, ED). The three formulations could be arranged in a descending order in  
370 relation to the percentage of total skin retention after 24 h as follows: ME (11.87%) >  
371 ESBG (4.74%) > cream (3.41%) (Table 4). As depicted in Fig. 6, there was no  
372 significant difference between ESBG and AZA cream after 24 h application ( $P > 0.5$   
373 for both SC data and ED data). However, the drug content in the skin layers  
374 (both in SC and viable skin layers) treated with the optimized ME was  
375 significantly higher compared to cream suspension ( $P < 0.01$ ) and ESBG ( $P$   
376  $< 0.05$ ), which was inconsistent with the permeation tendency through the  
377 skin.

378 As AZA was water insoluble, it could not completely dissolve in the cream and  
379 mainly suspended in this dosage form.<sup>5</sup> However, in the optimal ME and ESBG, AZA  
380 mainly existed in dissolved form due to their co-solvent and physicochemical  
381 properties. In generally, only the dissolved fraction of an active agent in a vehicle  
382 could enter the skin.<sup>32</sup> Therefore, both the optimal ME and ESBG resulted in  
383 significantly higher skin permeability than commercial cream. For AZA retention in  
384 skin layers, however, ESBG as well as cream resulted in significantly  
385 lower amount than the optimal ME, which be ascribed to the microstructure  
386 of MEs.

### 387 **3.6. Attenuated total reflectance fourier transform infrared spectroscopy** 388 **(ATR-FTIR) study**

389 ATR-FTIR study was conducted to study the skin-vehicle interaction and reveal  
390 the mechanism of enhanced cutaneous penetration based on various vehicles. In IR  
391 spectra of skin treated different formulation and untreated (control), the changes in  
392 peak position and intensity (peak height) of bands were compared, including CH<sub>2</sub>  
393 stretching (around 2924 cm<sup>-1</sup>, represent the asymmetric stretching CH<sub>2</sub> vibrations) and  
394 amide 1 stretching (around 1653 cm<sup>-1</sup>, sensitive to H-bond change in the SC).<sup>25,33</sup>

395 The change in peak intensity of band was considered to be important because it  
396 provided information about the lipid amount presenting in the SC. As shown in Fig. 7,  
397 after the treatment with ME, the peak height of CH<sub>2</sub> stretching (around  
398 2924 cm<sup>-1</sup>, 0.82%) was significantly increased compared to control (0.77%),  
399 implying lipid extraction in SC and enhancement in drug cutaneous

400 permeation;<sup>25</sup> while the SC treated with ESBG and cream displayed decreased  
401 peak intensity (0.73% for ESBG and 0.42% for cream), suggesting lipid  
402 strengthening in SC and subsequently significant retardation effect on  
403 percutaneous transport. Analysis of amide 1 model pointed to a shift to higher  
404 wavenumber when SC treated with ME (from 1653.40 to 1657.32  $\text{cm}^{-1}$ ) and ESBG  
405 (from 1653.40 to 1656.32  $\text{cm}^{-1}$ ) relative to untreated SC. The shift indicated the  
406 weakening of the H-bonds between the amide linkages within the SC, which favored  
407 substance penetration into skin.<sup>25</sup> The region corresponding to  $\text{CH}_2$  asymmetric  
408 vibration (around 2924  $\text{cm}^{-1}$ ) provided information about conformational order of the  
409 SC lipid chains.<sup>34</sup> After treated with ME formulation, the band shifted to higher values  
410 in comparison with control, suggesting the permeation enhancement due to disorder in  
411 the lipid arrangement. However, the band of SC treated with ESBG showed a shift to  
412 lower values, supporting the enhancement of stable organization of lipids.

### 413 **3.7. Skin irritation test**

414 Although most of the ingredients used in ME preparation were  
415 pharmaceutically approved, they might also irritate the skin at higher  
416 concentrations.<sup>35</sup> As a result, histopathological examination was performed  
417 to valuate any irritant potential of the optimized ME compared to control  
418 formulations.<sup>36</sup> After 3 days, rats in all the groups showed no apparent  
419 edema, erythema and other irritant response. Microscopic images of rat  
420 skin treated with various formulations were shown in Fig. 8. Compared to  
421 normal skin (Fig. 8a), the SC layer of rat skin treated with ME and ESBG

422 became thinner but without any apparent change in epidermis and dermis  
423 (Fig. 8c, d). Besides, the SC, epidermis and dermis layers were normal  
424 following cream application (Fig. 8b). In addition, the skin treated with  
425 cream, ESG and ME showed no sign of inflammation cells. The result  
426 suggested that the optimized ME might be safe to be used for topical AZA  
427 delivery.

### 428 **3.8. Pharmacodynamics studies**

429 Cutaneous polymorphonuclear leukocyte inflammation was induced by croton  
430 oil to evaluate the therapeutic effect of ME formulation on rosacea based on reduced  
431 ear redness, edema, et al.<sup>27,28</sup> Mice untreated (group f) and treated with croton  
432 oil only (group a) were used as negative and positive control,  
433 respectively. Croton oil could produce intense redness, accompanied by large  
434 number of infiltrated inflammatory cells in viable skin layers, edema, and even severe  
435 skin ulcer (Fig. 9a). The application of blank ME4 could not improve inflammation  
436 compared to positive control ear (Fig. 9a, b). On the contrary, AZA-loaded ME  
437 exhibited significant inhibitory effect on inflammation response based on the  
438 significantly reduced number of inflammatory cells in the whole skin layers (Fig. 9d),  
439 which was superior to ESG and commercial cream treated ears (Fig. 9c,e). It seemed  
440 that there was no significant difference between AZA-loaded ME treated ear and  
441 negative control ear (Fig. 9f) in both macro photos and micro photos. In addition,  
442 the application of AZA-loaded ME (group d) also significantly inhibited the increase  
443 of the ear thickness (ear edema) compared to the other formulations ( $P < 0.01$  for

444 group a,b;  $P < 0.05$  for group c, e) (Fig. 10). The results indicated that the optimized  
445 ME formulation significantly improved the therapeutic effect compared to market  
446 cream.

447 AZA, a bioactive molecule used in many skin disorders, restrains its  
448 penetration across the stratum corneum due to poor bioavailability mainly  
449 caused by low drug solubility and poor skin permeability. In order to  
450 enhance AZA solubility in the vehicles, ionization and monosodium salt  
451 of AZA were investigated, respectively.<sup>5,37</sup> In our study, however, AZA was  
452 completely solubilized in the optimal ME without any physical or chemical  
453 treatment. Besides, gel<sup>3</sup>, liquid crystal<sup>38</sup> and nanoscale vehicles  
454 (including microemulsion<sup>37</sup>, ethosomes and liposomes<sup>39</sup>) were developed as  
455 alternative topical formulations of AZA. In these studies, the effect of  
456 developed vehicles on the cutaneous permeation of AZA was investigated  
457 only using excised skin model in *in vitro* study. However, the therapeutic  
458 efficacy of AZA based on topical vehicles has to be proven, since there  
459 are many other variables that could affect the efficacy when used *in vivo*.  
460 Thus, in our study, *in vivo* pharmacodynamics studies were further  
461 conducted. The results indicated that the optimized ME formulation  
462 containing AZA significantly improved the therapeutic effect on rosacea.

463 Both metronidazole (MTZ) and AZA are considered to be the first-line  
464 treatment of rosacea. In our previous work, we have developed and  
465 optimized a ME to enhance targeting localization of MTZ in skin layers

466 and improve therapeutic efficacy of MTZ.<sup>27</sup> However, some comparative  
467 researches demonstrated that AZA was superior to MTZ in improving  
468 inflammatory lesions and erythema of rosacea.<sup>2</sup> Generally speaking, there  
469 were three obvious differences between these two research articles.  
470 Firstly, MTZ, with logP value of -0.18, shows highly hydrophilic property,  
471 resulting in limited permeation into and through the skin caused by  
472 lipophilic barrier of SC; while AZA is a lipophilic drug (logP value is  
473 1.45) and restrains skin penetration mainly due to its poor solubility.  
474 Secondly, considering significantly different properties between MTZ and  
475 AZA, we developed oil-in-water (O/W) ME for MTZ and water-in-oil (W/O)  
476 ME for AZA, respectively. The components of W/O ME in this study were also  
477 different from that of O/W ME in our previous study. Last but not least,  
478 in addition to the similar optimization and pharmacodynamics studies in  
479 our both studies, ATR-FTIR was further carried out to investigate the  
480 molecular vibrations of the SC components and reveal the mechanism of  
481 enhanced cutaneous penetration based on ME vehicle in current study.

482 In addition, porcine skin was chosen as *in vitro* penetration model in our study  
483 not only due to its physiological, biochemical and histological similarities to human  
484 skin, but also because of less variability than other skin models.<sup>40,41</sup> In contrast, the  
485 skin model from mice exhibited an extremely high density of hair follicles which  
486 might affect precutaneous absorption of molecules. Thus, hairy rodent skin is usually  
487 used in *in vivo* studies rather other *in vitro* studies.<sup>40</sup> Nevertheless, *in vivo* studies are



488 still performed on this specie. We realized the potential limitations caused by different  
489 animal models used for *in vitro* (porcine skin) and *in vivo* (mice). However, the  
490 optimal therapeutic effect of the optimal ME on rosacea might indicate the improved  
491 AZA retention in mice skin, demonstrating that these two models may have good  
492 correlations for the permeation of AZA to a certain degree.

#### 493 **4. Conclusion**

494 In current study, the application of ME systems for topical delivery of AZA was  
495 investigated. D-optimal mixture experimental design was applied to rapidly obtain the  
496 optimal AZA-loaded ME formulation realizing maximum skin accumulation,  
497 appropriate penetration into receptor medium and globule size. The optimal ME  
498 composed of 50.3% Smix (a mixture of Span 20/Ethanol, 1:9, w/w), 13.5% water and  
499 36.2% Capryol 90. Contrary to ESBG and commercial cream, the optimized ME  
500 significantly enhanced AZA retention in the skin and penetration through the skin in  
501 *in vitro* permeation studies. ATR-FTIR study indicated that the improved AZA release  
502 from the optimal ME was mainly due to the disturbed SC barrier function via lipid  
503 extraction, weakening H-bond between the amide linkages and disordering lipid  
504 arrangement of SC. Additionally, the results of skin irritation test and  
505 pharmacodynamics study inferred that the AZA-loaded optimized ME formulation  
506 was safe and more effective in the treatment of croton oil-induced rosacea than  
507 commercial cream and ESBG. Taken together, the optimal W/O ME might be a  
508 promising topical vehicle of AZA for improved therapeutic effect of anti-rosacea.

#### 509 **Acknowledgment**

510 We acknowledge the National Basic Research Project (2014CB932200) of the  
511 MOST for financial support.

512 **Declaration of Interest section**

513 The authors report no declarations of interest.

514 **References**

- 515 1. G.H. Crawford, M.T. Pelle, W.D. James, *J. Am. Acad. Dermatol.* 2004, 51, 327.
- 516 2. Y. Tuzun, R. Wolf, Z. Kutlubay, O. Karakus, B. Engin, *Clin. Dermatol.* 2014, 32,  
517 35.
- 518 3. K. Yamasaki, R. Gallo, *J. Dermatol. Sci.* 2009, 55, 77.
- 519 4. N. Li, Q. Su, F.P. Tan, J. Zhang, *Int. J. Pharm.* 2010, 387, 167.
- 520 5. N. Li, X.H. Wu, W.B. Jia, M.C. Zhang, F.P. Tan, J. Zhang, *Drug. Dev. Ind. Pharm.*  
521 2012, 38, 985-994.
- 522 6. S.A. Fouad, E.B. Basalious, M.A. El-Nabarawi, S.A. Tayel, *Int. J. Pharm.* 2013,  
523 453, 569.
- 524 7. Y. Yang, R.M. Pearson, O. Lee, C.W. Lee, R.T. Chatterton, S.A. Khan, S. Hong,  
525 *Adv. Funct. Mater.* 2014, 27, 2442.
- 526 8. N. Li, W.B. Jia, Y. Zhang, F.P. Tan, J. Zhang, *Int. J. Pharm.* 2011, 415, 169.
- 527 9. G. Cevc, U. Vierl, *J. Control. Release.* 2010, 141, 277.
- 528 10. T. Bhuvaneswari, M. Thiyagarajan, N. Geetha, P. Venkatachalam, *Acta. Trop.*  
529 2014, 135, 55.
- 530 11. W.W. Gao, D. Vecchio, J.M. Li, J.Y. Zhu, Q.Z. Zhang, V. Fu, J.Y. Li, S.  
531 Thamphiwatana, D.N. Lu, L.F. Zhang, *ACS. NANO.* 2014, 8, 2900.

- 532 12. G. Gainza, M. Pastor, J.J. Aguirre, S. Villullas, J.L. Pedraz, R.M. Hernandez, M.  
533 Igartua, *J. Control. Release.* 2014, 85, 51.
- 534 13. S. Sahoo, N.R. Pani, S.K. Sahoo, *Colloid. Surface. B.* 2014, 120, 193.
- 535 14. H. X. Ma, M. Yu, M. Z. Lei, F. P. Tan, N. Li, *AAPS PharmSciTech.* DOI:  
536 10.1208/s12249-014-0278-5.
- 537 15. D. Pepe, M. McCall, H. Zheng, L. B. Lopes, *J. Pharm. Sci.* DOI:  
538 10.1002/jps.23482.
- 539 16. F. T. M. C. Vicentini, T. R. M. Simi, J. O. Del Ciampo, N. O. Wolga, D. L.  
540 Pitol, M. M. Iyomasa, M. V. L. B. Bentley, M. J. V. Fonseca, *Eur. J. Pharm.*  
541 *Biopharm.* 2008, 69, 948.
- 542 17. L. M. P. D. Araujo, J. A. Thomazine, R. F. V. Lopez, *Eur. J. Pharm. Biopharm.* 2010,  
543 75, 48.
- 544 18. M. Kreilgaard, *Adv. Drug. Deliver. Rev.* 2002, 54, S77.
- 545 19. M. J. Lawrence, G. D. Rees, *Adv. Drug. Deliv. Rev.* 2012, 64, 175.
- 546 20. M. Fanun, *Curr. Opin. Colloid. In.* 2012, 17, 306.
- 547 21. Y. H. Tsai, F. K. Lee, Y. B. Huang, C. T. Huang, P. C. Wu, *Int. J. Pharm.* 2010, 388,  
548 257.
- 549 22. F. T. M. Vicentini, T. R. M. Simi, J. O. Del Ciampo, N. O. Wolga, D. L. Pitol, M. M.  
550 Iyomasa, M. V. L. B. Bentley, M. J. V. Fonseca, *Eur. J. Pharm. Biopharm.* 2008, 69, 948.
- 551 23. A. S. B. Goebel, U. Knie, C. Abels, J. Wohlrab, R. H. H. Neubert, *Eur. J. Pharm.*  
552 *Biopharm.* 2010, 75, 162.
- 553 24. Y. B. Huang, Y. H. Tsai, W. C. Yang, J. S. Chang, P. C. Wu, K. Takayama,

- 554 Eur. J. Pharm. Biopharm. 2004, 58, 607.
- 555 25. D. Kaushik, B. Michniak-Kohn, AAPS PharmSciTech. 2010, 11, 1068.
- 556 26. N. Aggarwal, S. Goindi, R. Khurana, Colloid. Surface. B. 2013,105,158.
- 557 27. M. Yu, H.X. Ma, M.Z. Lei, N. Li, F.P. Tan, Eur. J. Pharm. Biopharm. 2014, 88, 92.
- 558 28. J.X. Zhang, X.Y. Xu, N.V. Rao, B. Argyle, L. McCord, W.J. Rusho, T.P. Kennedy,  
559 G.D. Prestwich, G. Krueger, Plos One 2011, 6, e16658.
- 560 29. H. K. Patel, B. S. Barot, P. K. Shelat, A. Shukla, Colloids. Surf. B.  
561 Biointerfaces. 2013, 102, 86.
- 562 30. A.C. Sintov, I. Greenberg, Int. J. Pharm. 2014, 471, 516.
- 563 31. A.C. Sintov, L. Shapiro, J. Control. Release. 2004, 95, 173.
- 564 32. A.H. Elshafeey, A.O. Kamel, M.M. Fathallah, Pharm. Res. 2009, 26, 2446.
- 565 33. G. Rodriguez, L. Barbosa-Barros, L. Rubio, M. Cocera, A. Diez, J.  
566 Estelrich, R. Pons, J. Caelles, A.D.L. Maza, O. Lopez, Langmuir.  
567 2009, 25, 10595.
- 568 34. S.M. Ge, Y.Y. Lin, H.Y. Lu, Q., J. He, B. Chen, C.B. Wu, Y.H. Xu. Int. J. Pharm.  
569 2014, 465, 120.
- 570 35. F.F. Sahle, J. Wohlrab, R.H.H. Neubert, Eur. J. Pharm. Biopharm. 2014, 86, 244.
- 571 36. N. Ü. Okur, Ş. Apaydın, N. Ü. K. Yavaşoğlu, A. Yavaşoğlu, H. Y. Karasulu,  
572 Int. J. Pharm. 2011, 46, 136.
- 573 37. E. Peira, M.E. Carlotti, R. Cavalli, M. Trotta, J. Drug. Deliv. Sci.  
574 Tec. 2006, 16, 375.
- 575 38. F. Aytekin, R.N. Gursoy, S. Ide, E.H. Soylu, S. Hekimoglu, Drug. Dev.

- 576 Ind. Pharm. 2013, 39, 228.
- 577 39. E. Esposito, E. Menegatti, R. Cortesi, Int. J. Cosmetic. Sci. 2004,  
578 26, 270.
- 579 40. B. Godin, E. Touitou, Adv. Drug. Deliv. Rev. 2007, 59, 1152.
- 580 41. F.C. Rossetti, L.B. Lopes, A.R.H. Carollo, J.A. Thomazini, A.C. Tedesco,  
581 M.V.L.B. Bentley, J. Control. Release. 2011, 55, 400.
- 582
- 583
- 584
- 585
- 586
- 587
- 588
- 589
- 590
- 591
- 592
- 593
- 594
- 595
- 596
- 597

598 **Table 1**

599 The formulations of mixture design and their characterization results.

No.	Smix (X <sub>1</sub> )	Water (X <sub>2</sub> )	Oil (X <sub>3</sub> )	Skin retention (µg) (Y <sub>1</sub> )	AZA amount in collection medium at 24 h (µg) (Y <sub>2</sub> )	Particle size (nm) (Y <sub>3</sub> )
1	68.27	3.49	28.24	317.86	353.42	0
2	80	0	20	202.91	261.67	0
3	65.37	14.63	20	403.56	663.65	9
4	40	9.81	50.19	289.17	472.65	1.48
5	80	0	20	202.91	161.67	0
6	53.98	13.59	32.43	593.26	573.95	4.36
7	50.49	0	49.51	120.67	193.38	0
8	53.98	13.59	32.43	591.47	583.93	4.36
9	65.37	14.63	20	503.56	663.65	8.55
10	50	30	20	543.89	792.74	12
11	40	0	60	111.49	222.33	0
12	40	20.28	39.72	385.43	520.91	7.75
13	40	0	60	123.67	246.30	0
14	40	30	30	514.58	699.58	12
15	60.32	0	39.68	214.40	327.17	0
16	60.32	0	39.68	234.45	359.23	0

600

601

602

603

604

605

606

607

608

609 **Table 2**

610 Model summary statistics of the measured response.

Response	Model	SD	R <sup>2</sup>	Adjusted R <sup>2</sup>	PRESS
Y1	Linear	95.18	0.7362	0.6957	161000
	Quadratic	69.83	0.8908	0.8362	104600
	Special cubic	34.37	0.9762	0.9603	31320.77
	Cubic	40.45	0.9780	0.9450	575200
Y2	Linear	83.69	0.8305	0.7655	145400
	Quadratic	51.00	0.9580	0.9371	65780.87
	Special cubic	52.97	0.9593	0.9321	71972.51
	Cubic	57.44	0.9681	0.9202	1726000
Y3	Linear	1.34	0.9274	0.9162	32.66
	Quadratic	1.19	0.9556	0.9335	48.09
	Special cubic	1.01	0.9714	0.9523	39.18
	Cubic	0.32	0.9980	0.9951	64.77

611

612

613

614

615

616

617

618

619

620

621

622

623 **Table 3**

624 Predicted and experimental values for the optimized microemulsion.

625

Response	Predicted value	Experimental values	Error % <sup>a</sup>
Y <sub>1</sub>	571.64	593.57	3.69
Y <sub>2</sub>	573.97	584.69	1.83
Y <sub>3</sub>	3.78	3.83	1.32

626 <sup>a</sup> Error% was calculated using the formula [(Experimental value - Predicted  
627 value)/Experimental value] × 100

628

629

630

631

632

633

634

635

636

637

638

639

640



641 Table 4

642 pH value and the permeation parameters of commercial cream, ESBG and the  
643 optimized ME formulation.

Formulation	pH value	Flux ( $\mu\text{g}/\text{cm}^2 \text{ h}$ )	Amount in collection medium at 24 h ( $\mu\text{g}$ )	ER	Total skin retention (%)
Cream	$3.44 \pm 0.052$	$4.29 \pm 0.23$	$129.48 \pm 14.56$	--	$3.41 \pm 0.31$
ESBG	$3.13 \pm 0.058$	$10.73 \pm 2.68^*$	$401.875 \pm 26.99^*$	3.10	$4.74 \pm 0.35$
ME	$4.15 \pm 0.071$	$15.64 \pm 2.49^{**}$	$584.69 \pm 40.87^{**}$	4.52	$11.87 \pm 0.76^{**}$

644

645 ER: enhancement ratio for drug permeation=Flux in ESBG or ME/Flux in cream.

646 \*  $P < 0.05$ , when compared to control

647 \*\*  $P < 0.01$ , when compared to control

648

649

650

651

652

653

654

655

656

657

658

659 Table 5

660 Storage stability of AZA ME under long-term condition. Data represent mean  $\pm$  SD  
661 for three batches.

Parameters	M <sup>a</sup> 0	M <sup>a</sup> 1	M <sup>a</sup> 2	M <sup>a</sup> 3
Appearance	Transparent	Transparent	Transparent	Transparent
Droplet size (nm)	3.83 $\pm$ 0.071	3.92 $\pm$ 0.095	3.98 $\pm$ 0.083	4.15 $\pm$ 0.075
PDI	0.216 $\pm$ 0.002	0.198 $\pm$ 0.003	0.295 $\pm$ 0.004	0.167 $\pm$ 0.003

662 <sup>a</sup>M stands for month

663

664

665

666

667

668

669

670

671

672

673

674

675

676

677

**Figure captions**

**Fig. 1** Pseudo-ternary phase diagram showing a w/o microemulsion region (area surrounded by pink line) made of Capryol 90 (oil phase), water, and the mixture of Span 20 (surfactant) and ethanol (cosurfactant) at a fixed mass ratio of 1:9. Area surrounded by blue line was used for D-optimal design.

**Fig. 2** 2D contour plots for the effects of variables on the skin retention after 24 h ( $\mu\text{g}$ ) (a), AZA amount in collection medium after 24 h ( $\mu\text{g}$ ) (b) and particle size (nm) (c) of W/O ME.

**Fig. 3** Overlay plot for the effect of different variables on the three responses: skin retention after 24 h ( $\mu\text{g}$ ) ( $Y_1$ ), AZA amount in collection medium after 24 h ( $\mu\text{g}$ ) ( $Y_2$ ) and particle size (nm) ( $Y_3$ ).

**Fig. 4** Typical appearance and particle size distribution of the optimal ME formulation.

**Fig.5** Permeated amount of AZA in the receptor medium at various time points: comparison of commercial cream, ESBG and the optimal ME. Results are expressed as mean  $\pm$  SD, n = 6. \* p < 0.05, \*\* p < 0.01.

**Fig.6** Percentage amount of azelaic acid distributed in stratum corneum (SC), epidermis and dermis (ED) after 24 h exposure of commercial cream, ESBG and the optimal ME. Results are expressed as mean  $\pm$  SD, n = 6. \* p < 0.05, \*\* p < 0.01.

**Fig.7** Representative ATR-FTIR spectra of untreated porcine skin SC (control) and SC treated with the optimal ME, ESBG and commercial cream.

**Fig.8** Microscopic images of rat skin treated with (a) normal saline, (b) commercial cream, (c) ESBG and (d) the optimal ME.

**Fig. 9** Photomicrograph of mice ears (upper panel), H&E-stained mice ear tissue at a magnification of  $10 \times$  (middle panel) and magnification of  $20 \times$  (bottom panel) sensitized with

various formulations. Mice ear treated with (a) croton oil, (b) croton oil and blank ME, (c) croton oil and drug loaded ESG, (d) croton oil and drug loaded ME, (e) commercial cream. And mice ear untreated used as control (f).The number 1 indicated inflammatory cells. The number 2 and number 3 indicated skin ulcer and edema, respectively.

**Fig.10** Ear thickness differences between left (untreated) and right (treated) ears of mice treated with different formulations respectively.

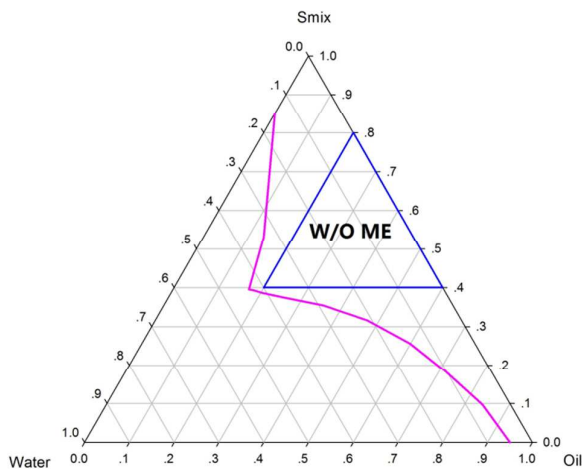


**Fig. 1** Pseudo-ternary phase diagram showing a w/o microemulsion region (area surrounded by pink line) made of Capryol 90 (oil phase), water, and the mixture of Span 20 (surfactant) and ethanol (cosurfactant) at a fixed mass ratio of 1:9. Area surrounded by blue line was used for D-optimal design.

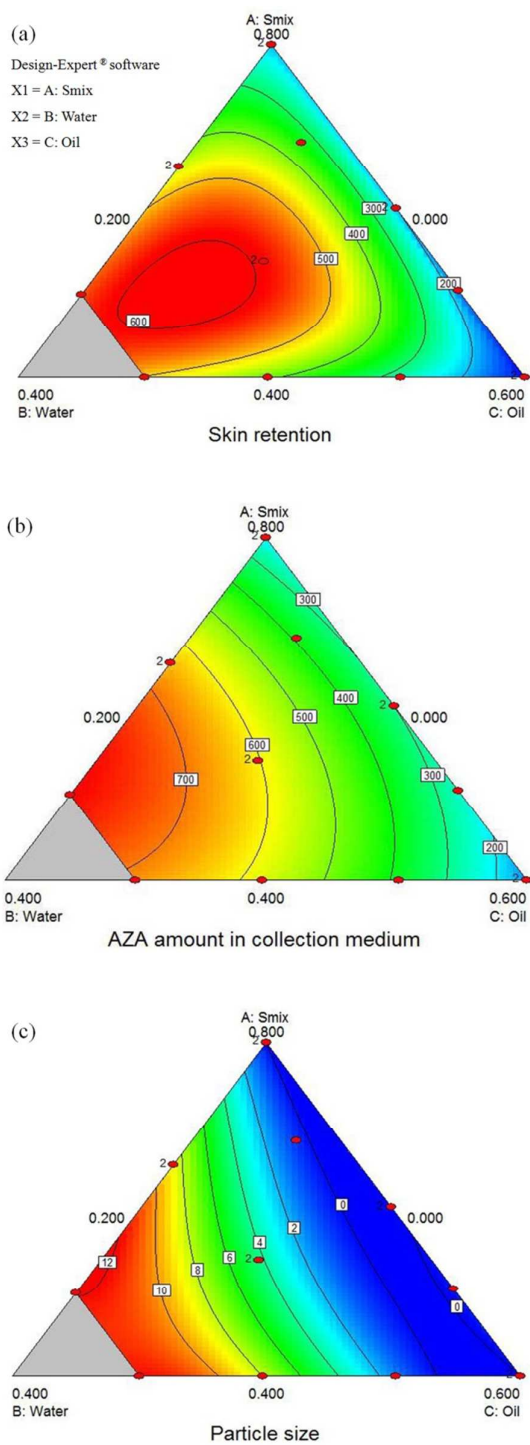


**Fig. 2** 2D contour plots for the effects of variables on the skin retention after 24 h ( $\mu\text{g}$ ) (a), AZA amount in collection medium after 24 h ( $\mu\text{g}$ ) (b) and particle size (nm) (c) of W/O ME.

Design-Expert® software

X1 = A: Smix

X2 = B: Water

X3 = C: Oil

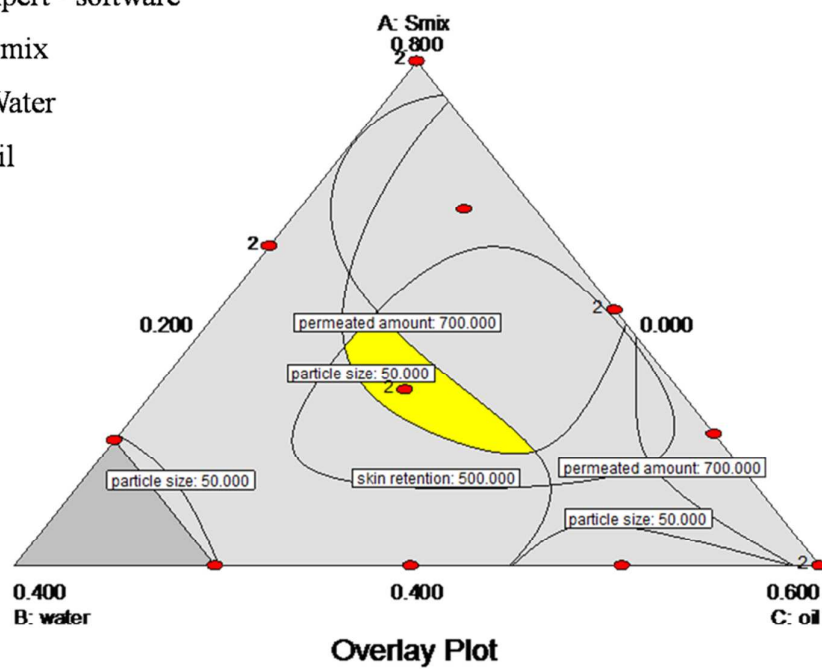


**Fig. 3** Overlay plot for the effect of different variables on the three responses: skin retention after 24 h ( $\mu\text{g}$ ) ( $Y_1$ ), AZA amount in collection medium after 24 h ( $\mu\text{g}$ ) ( $Y_2$ ) and particle size (nm) ( $Y_3$ ).

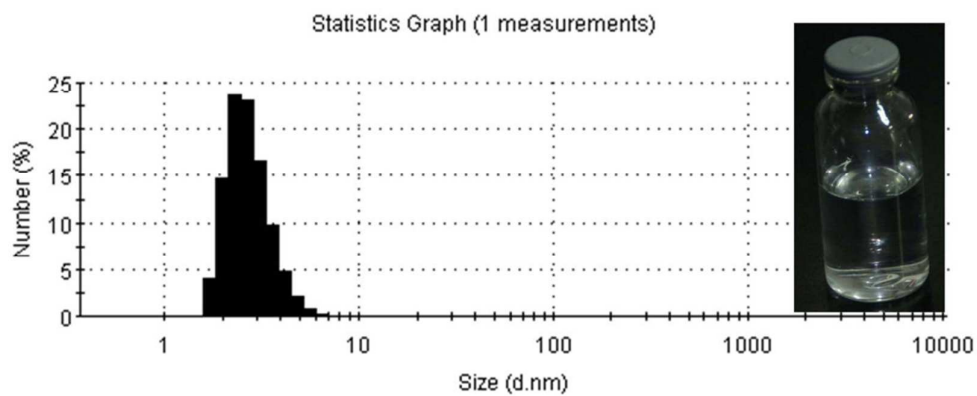


**Fig. 4** Typical appearance and particle size distribution of the optimal ME formulation.



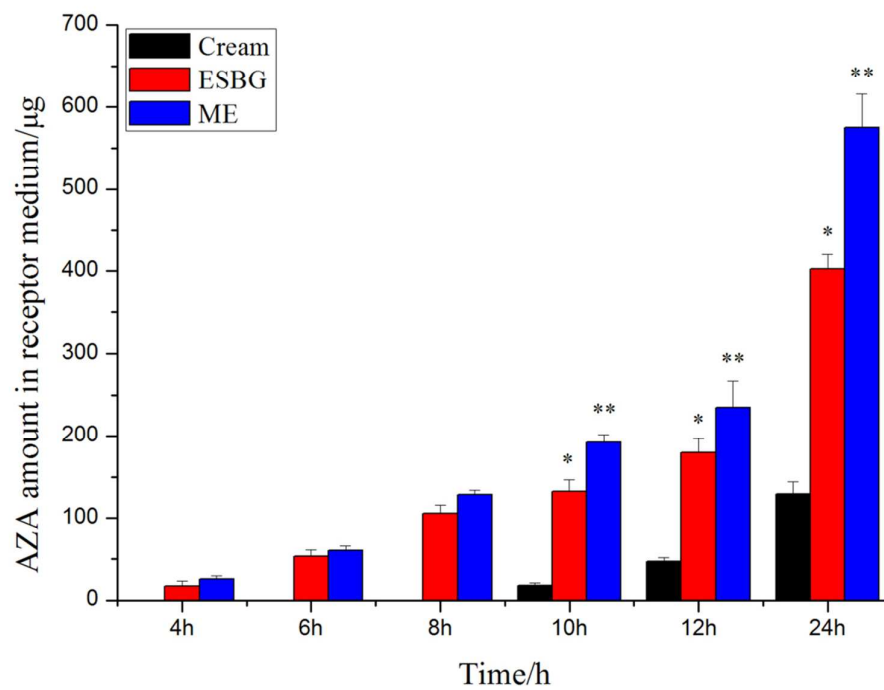


**Fig.5** Permeated amount of AZA in the receptor medium at various time points: comparison of commercial cream, ESG and the optimal ME. Results are expressed as mean  $\pm$  SD, n = 6. \* p < 0.05, \*\* p < 0.01.

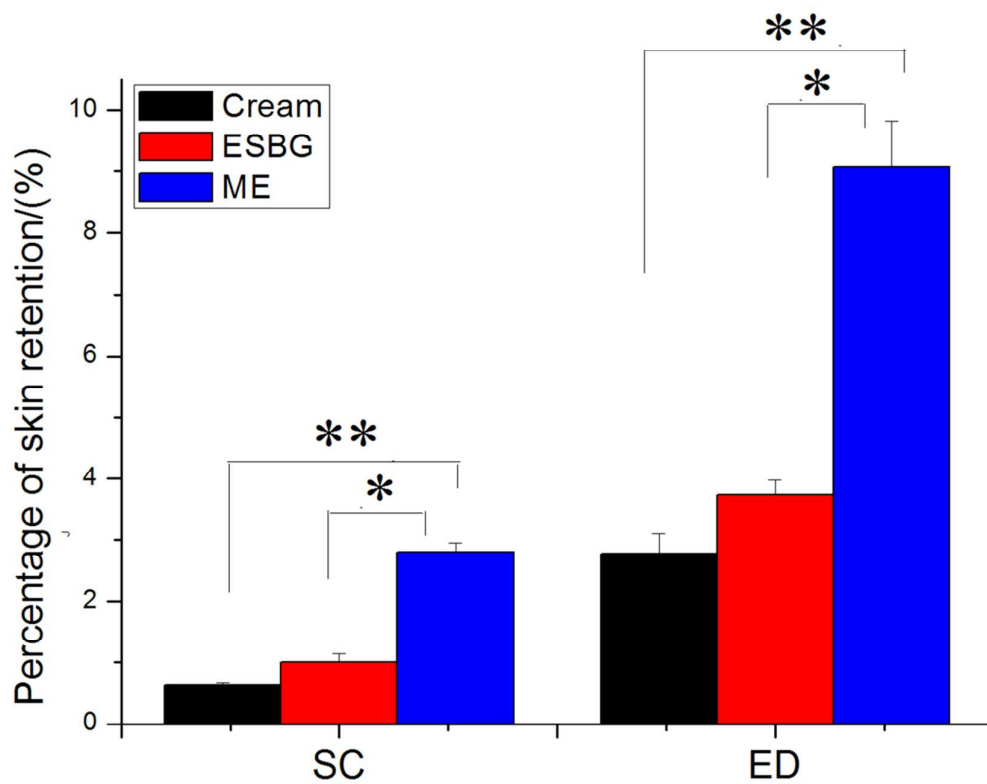


**Fig.6** Percentage amount of azelaic acid distributed in stratum corneum (SC), epidermis and dermis (ED) after 24 h exposure of commercial cream, ESBG and the optimal ME. Results are expressed as mean  $\pm$  SD, n = 6. \* p < 0.05, \*\* p < 0.01.

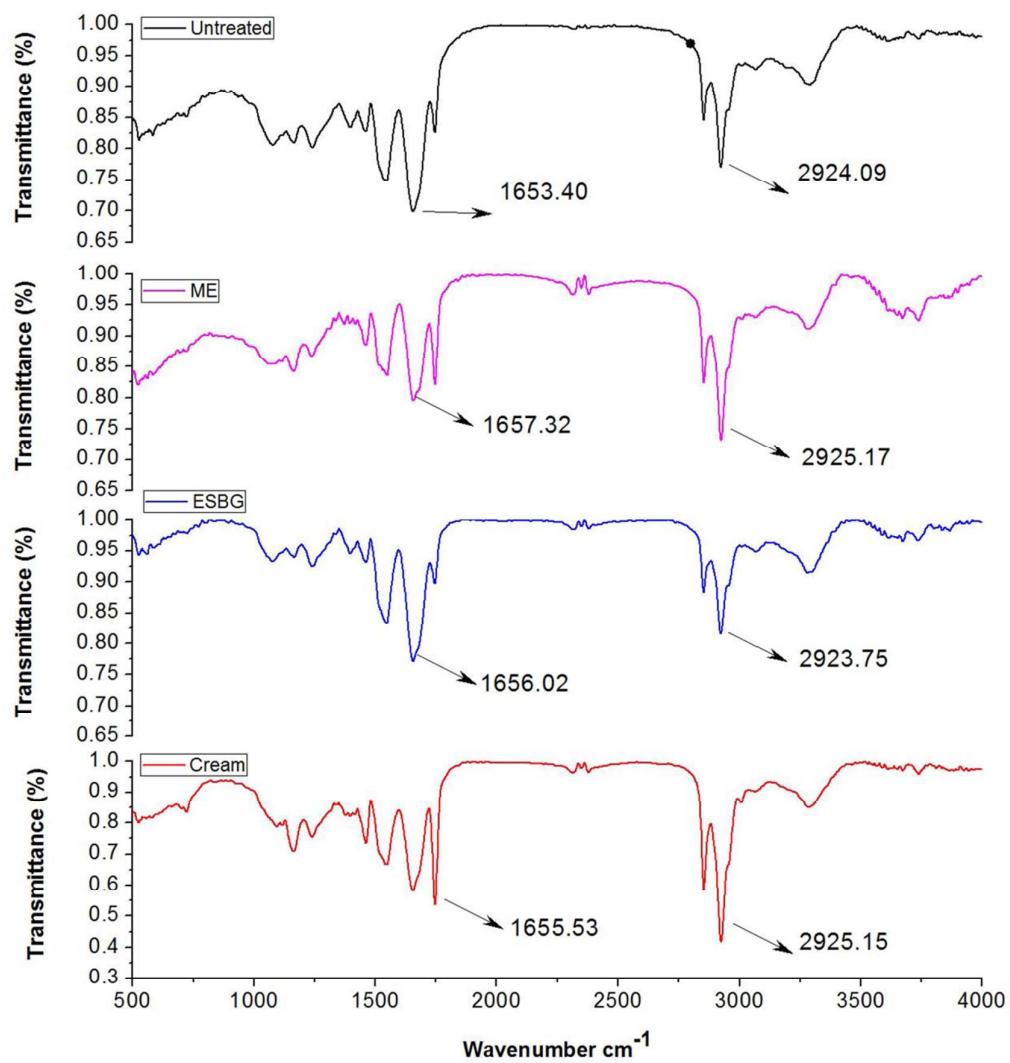


**Fig.7** Representative ATR-FTIR spectra of untreated porcine skin SC (control) and SC treated with the optimal ME, ESBG and commercial cream.

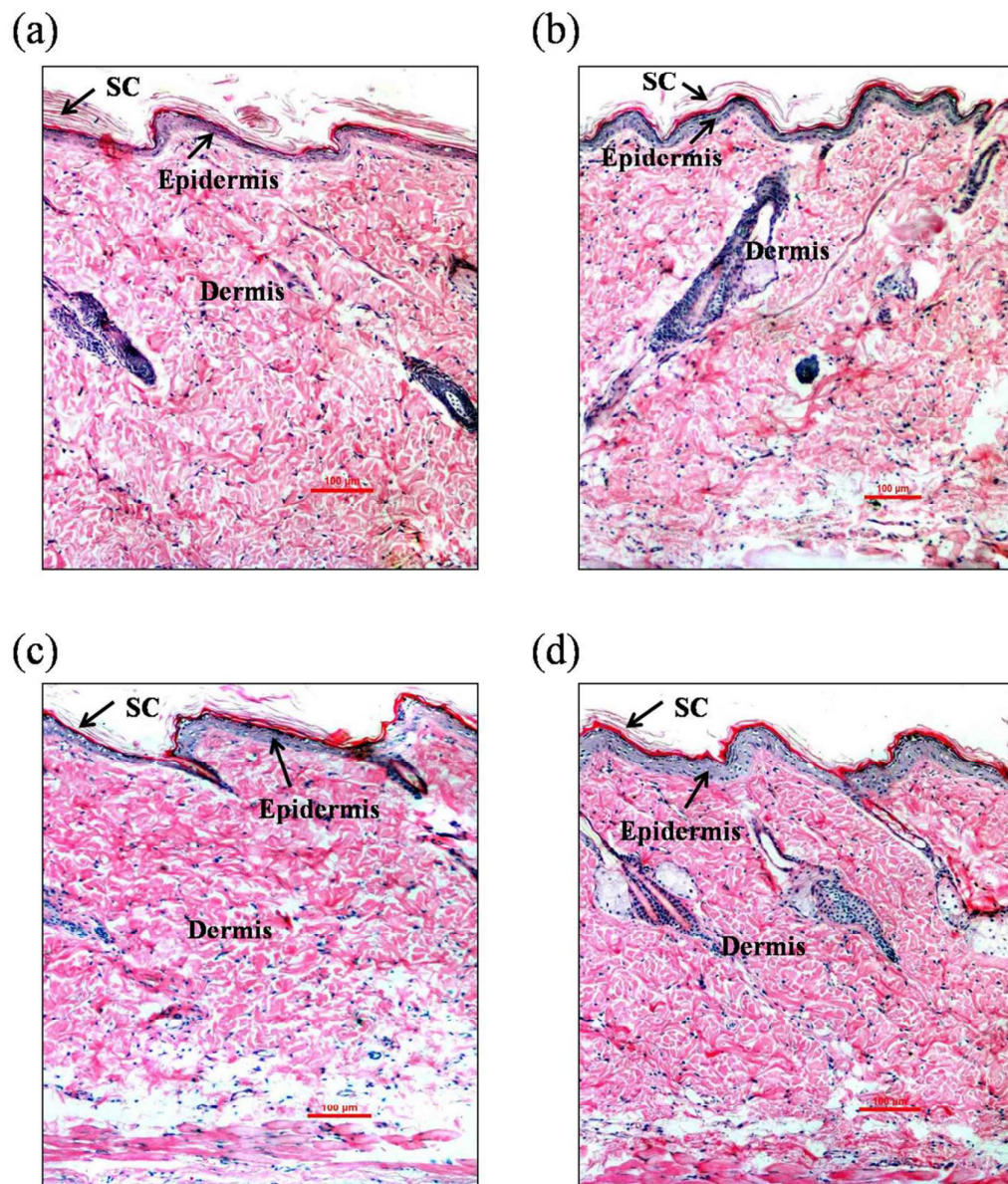


**Fig.8** Microscopic images of rat skin treated with (a) normal saline, (b) commercial cream, (c) ESBG and (d) the optimal ME.

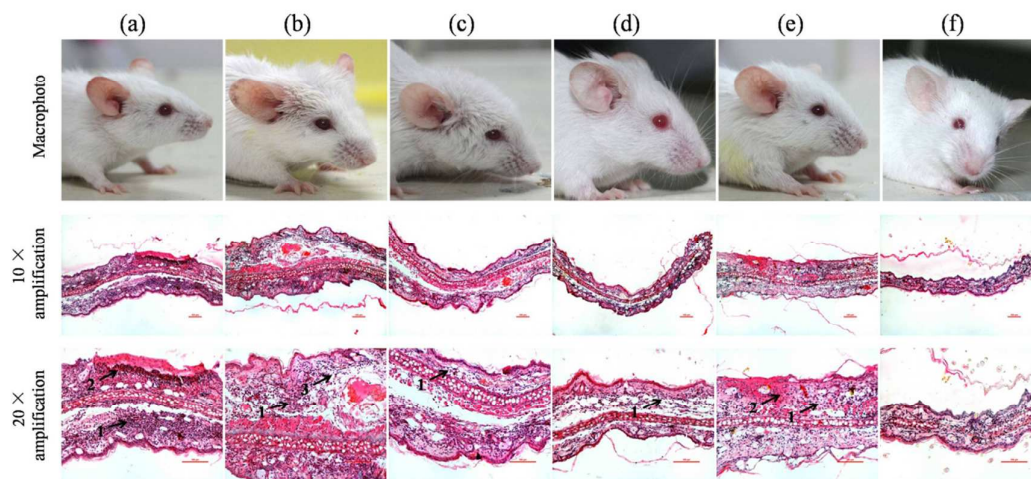


**Fig. 9** Photomicrograph of mice ears (upper panel), H&E-stained mice ear tissue at a magnification of  $10 \times$  (middle panel) and magnification of  $20 \times$  (bottom panel) sensitized with various formulations. Mice ear treated with (a) croton oil, (b) croton oil and blank ME, (c) croton oil and drug loaded ESBG, (d) croton oil and drug loaded ME, (e) commercial cream. And mice ear untreated used as control (f). The number 1 indicated inflammatory cells. The number 2 and number 3 indicated skin ulcer and edema, respectively.

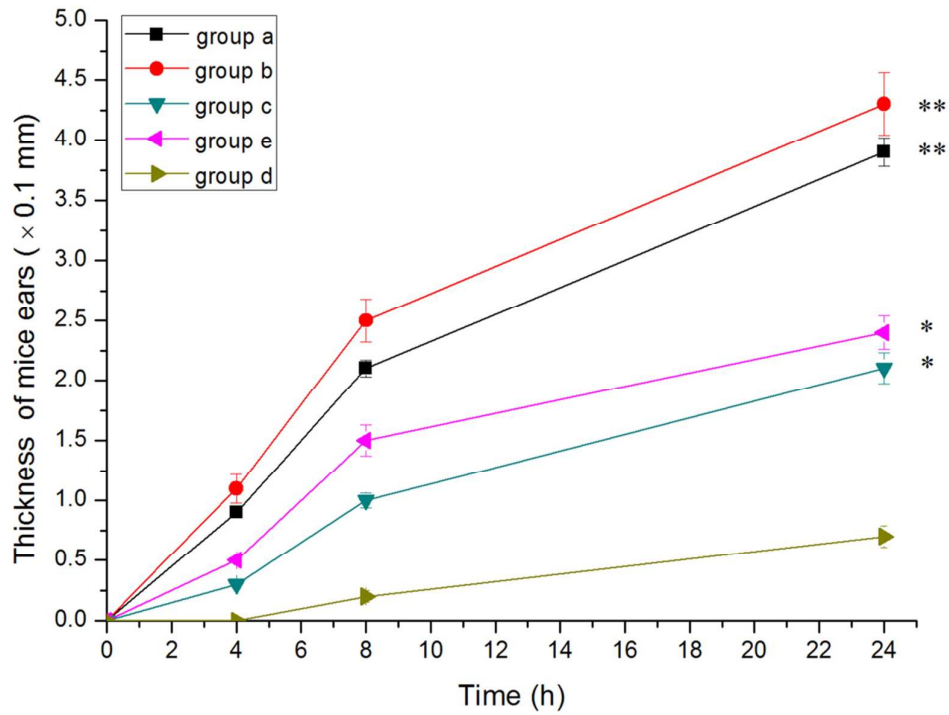


**Fig.10** Ear thickness differences between left (untreated) and right (treated) ears of mice treated with different formulations respectively.